



CHALMERS

Chalmers Publication Library

Experimental Investigation and Modeling of the Throughput of a 2×2 Closed-Loop MIMO System in a Reverberation Chamber

This document has been downloaded from Chalmers Publication Library (CPL). It is the author's version of a work that was accepted for publication in:

IEEE Transactions on Antennas and Propagation (ISSN: 0018-926X)

Citation for the published paper:

Chen, X. (2014) "Experimental Investigation and Modeling of the Throughput of a 2×2 Closed-Loop MIMO System in a Reverberation Chamber". IEEE Transactions on Antennas and Propagation, vol. 62(9), pp. 4832-4835.

Downloaded from: <http://publications.lib.chalmers.se/publication/202414>

Notice: Changes introduced as a result of publishing processes such as copy-editing and formatting may not be reflected in this document. For a definitive version of this work, please refer to the published source. Please note that access to the published version might require a subscription.

Chalmers Publication Library (CPL) offers the possibility of retrieving research publications produced at Chalmers University of Technology. It covers all types of publications: articles, dissertations, licentiate theses, masters theses, conference papers, reports etc. Since 2006 it is the official tool for Chalmers official publication statistics. To ensure that Chalmers research results are disseminated as widely as possible, an Open Access Policy has been adopted. The CPL service is administrated and maintained by Chalmers Library.

(article starts on next page)

REFERENCES

- [1] K. Chang, R. York, P. Hall, and T. Itoh, "Active integrated antennas," *IEEE Trans. Microw. Theory Tech.*, vol. 50, no. 3, pp. 937–944, Mar. 2002.
- [2] D. Segovia-Vargas, D. Castro-Galán, L. E. García-Muñoz, and V. González-Posadas, "Broadband active receiving patch with resistive equalization," *IEEE Trans. Microw. Theory Tech.*, vol. 56, no. 1, pp. 56–64, Jan. 2008.
- [3] V. Radisic, Y. Qian, and T. Itoh, "Novel architectures for high-efficiency amplifiers for wireless applications," *IEEE Trans. Microw. Theory Tech.*, vol. 46, no. 11, pp. 1901–1909, Nov. 1998.
- [4] F. R. Hsiao, T. W. Chiou, and K. L. Wong, "Harmonic control of a square microstrip antenna operated at the 1.8 GHz band," in *Proc. Microw. Conf. Asia-Pacific*, Aug. 2001, pp. 1052–1055.
- [5] V. Radisic, S. T. Chew, Y. Qian, and T. Itoh, "High efficiency power amplifier integrated with antenna," *IEEE Microw. Guided Wave Lett.*, vol. 7, no. 2, pp. 39–41, Feb. 1997.
- [6] Y. Horii and M. Tsutsumi, "Harmonic control by photonic bandgap on microstrip patch antenna," *IEEE Microw. Guided Wave Lett.*, vol. 9, no. 1, pp. 13–48, Jan. 1999.
- [7] X. C. Lin and L. T. Wang, "A broadband CPW-Fed loop slot antenna with harmonic control," *IEEE Antennas Wireless Propag. Lett.*, vol. 2, no. 1, pp. 323–325, 2003.
- [8] A. S. Andrenko, Y. Ikeda, and O. Ishida, "Application of PBG microstrip circuits for enhancing the performance of high-density substrate patch antennas," *Microw. Opt. Technol. Lett.*, vol. 32, no. 5, pp. 340–344, Mar. 2002.
- [9] Y. J. Sung, M. Kim, and Y. S. Kim, "Harmonics reduction with defected ground structure for a microstrip patch antenna," *IEEE Antennas Wireless Propag. Lett.*, vol. 2, pp. 111–113, 2003.
- [10] S. Biswas, D. Guha, and C. Kumar, "Control of higher harmonics and their radiation in microstrip antennas using compact defected ground structures," *IEEE Trans. Antennas Propag.*, vol. 61, no. 6, pp. 3349–3353, Jun. 2013.
- [11] N. A. Nguyen, R. Ahmad, Y. T. Im, Y. S. Shin, and S. O. Park, "A T-shaped wide-slot harmonic suppression antenna," *IEEE Antennas Wireless Propag. Lett.*, vol. 6, pp. 647–650, 2007.
- [12] D. H. Choi, Y. J. Cho, and S. O. Park, "A broadband slot antenna with harmonic suppression," *Microw. Opt. Technol. Lett.*, vol. 48, no. 10, pp. 1984–1987, Oct. 2006.
- [13] N. Boissouvier, F. Le Bolzer, A. Louzir, A. C. Tarot, and K. Mahdjoubi, "Harmonic-less annular slot antenna (ASA) using a novel PBG structure for slot-line printed devices," in *Proc. IEEE Antennas Propag. Soc. Int. Symp.*, Jun. 2003, vol. 2, pp. 553–556.
- [14] D. J. Woo, T. K. Lee, J. W. Lee, C. S. Pyo, and W. K. Choi, "Novel U-slot and V-slot DGSs for bandstop filter with improved Q factor," *IEEE Trans. Microw. Theory Tech.*, vol. 54, no. 6, pp. 2840–2847, Jun. 2006.
- [15] K. L. Wong, C. C. Huang, and W. S. Chen, "Printed ring slot antenna for circular polarization," *IEEE Trans. Antennas Propag.*, vol. 50, no. 1, pp. 75–77, Jan. 2002.
- [16] J. S. Park, J. H. Kim, J. H. Lee, S. H. Kim, and S. H. Myung, "A novel equivalent circuit modeling method for defected ground structure and its application to optimization of a DGS lowpass filter," in *IEEE Int. Microw. Symp. Digest*, 2002, vol. 1, pp. 417–420.

Experimental Investigation and Modeling of the Throughput of a 2×2 Closed-Loop MIMO System in a Reverberation Chamber

Xiaoming Chen

Abstract—Throughputs of 2×2 long term evolution (LTE) multiple-input multiple-output (MIMO) systems in both open- and closed-loop configurations have been studied previously. However, in the previous work, the study of the closed-loop MIMO system is limited to receive semi-correlation (i.e., correlations exist only at the receive side only), resulting in inaccurate modeling of the closed-loop throughput with large transmit antenna correlations and incomplete conclusion about the effectiveness of codebook based precoding based on 2-bit feedback. In this work, the effect of the transmit antenna correlation on the closed-loop throughput is examined. Unlike in the previous work, an inversely weighted mean square error (MSE) matrix is proposed as the precoding selection criterion, resulting in good agreements between the simulations and the RC measurements of a closed-loop LTE system with various correlations. It is found that the closed-loop MIMO system is superior to its open-loop counterpart in the presence of large transmit antenna correlation in the low and medium signal-to-noise (SNR) regimes.

Index Terms—Long term evolution (LTE), multiple-input multiple-output (MIMO), reverberation chamber (RC), throughput.

I. INTRODUCTION

Reverberation chambers (RCs) have been used for various over-the-air (OTA) tests [1]–[6]. For instance, the RC has been used to measure the bit error rate (BER) of a communication system [1], [2] as well as the total radiated power (TRP) and the total isotropic sensitivity (TIS) of mobile terminals [3]; very recently, it has been used for measuring the throughputs (and the Electromagnetic immunity) of wireless local area network (WLAN) systems [4] and long term evolution (LTE) systems [5], [6]. Currently, there is a great interest in measuring the throughput of the LTE multiple-input multiple-output (MIMO) system. To complement the RC measurement, MIMO throughput models have been developed in [6]. Nevertheless, the study of the closed-loop MIMO system in [6] is confined to receive semi-correlation, resulting in inaccurate throughput modeling for closed-loop MIMO systems in the presence of correlations at the transmit side.

In this work, we focus on the closed-loop MIMO system and investigate correlations at both MIMO ends. To take the practical setting in the spatial multiplexing LTE system into account, an inversely weighted matrix (cf. Section II) is used in selecting the precoding matrix, instead of the unweighted precoding selection criterion in [6]. Although the throughput model is valid for any MIMO size, current OTA tests of MIMO systems are limited to 2×2 MIMO systems due to the fact that the current communication tester and LTE mobile phones have only two antenna ports. As a result, we choose the two-antenna codebook based on 2-bit feedback [7]. For the throughput measurement in the RC, we use the CITA good and bad reference antennas [8]

Manuscript received April 13, 2014; revised May 10, 2014; accepted June 06, 2014. Date of publication June 12, 2014; date of current version September 01, 2014.

The author is with the Chalmers University of Technology, Signals and Systems, Gothenburg, Sweden, 41296 (e-mail: xiaoming.chen@chalmers.se).

Color versions of one or more of the figures in this communication are available online at <http://ieeexplore.ieee.org>.

Digital Object Identifier 10.1109/TAP.2014.2330599

to introduce predefined antenna correlations at both MIMO ends. There are good agreements between the measured and modeled throughputs. Using the throughput model and RC measurements, we are able to study the effect of the channel correlation on the throughput performance of the closed-loop LTE MIMO system. In order to investigate the effectiveness of the codebook-based precoding in the closed-loop MIMO system, we conduct simulations and measurements of open-loop MIMO system and compare the throughputs of the open- and closed-loop MIMO systems. Results show that the codebook-based precoding is insensitive to receive antenna correlations but effective to the large transmit antenna correlation. The former observation results in the incomplete conclusion that codebook-based precoding has little effects on the throughput in [6]. In this work, in order to study the effectiveness of the codebook-based precoding, the throughput of the closed-loop MIMO system is compared with that of the open-loop MIMO system. It is shown that the closed-loop MIMO system is superior to its open-loop counterpart (in terms of throughput) in the presence of large correlation at the transmit side in the low and medium signal-to-noise (SNR) regimes. Explanations of these observations are given in Section III.

Notations: Throughout this communication, $*$, T , and H denote complex conjugate, transpose, and Hermitian operators, respectively. Lowercase letter (x), lowercase bold letter (\mathbf{x}), and uppercase bold letter (\mathbf{X}) represent scalar, column vector, and matrix, respectively. $\|\mathbf{x}\|_2$ denotes the 2-norm of \mathbf{x} . x_i and \mathbf{x}_i denote the i th element and column of \mathbf{x} and \mathbf{X} , respectively. E denotes the expectation and \mathbf{I} represents the identity matrix.

II. THROUGHPUT MODELING

Due to the heavy computational complexity of implementing the Turbo code in LTE systems [7], system simulations are usually limited to uncoded bit error rate (BER), e.g., [9], [10]. A simple way to include the Turbo code in a LTE system (or any other powerful channel code) is to use the threshold receiver model [11]: the block error rate (BLER) of a single-input single-output (SISO) system with a powerful channel code in an additive white Gaussian noise (AWGN) channel can be model as

$$P_e(\gamma) = \begin{cases} 1, & \gamma < \gamma_{th} \\ 0, & \gamma > \gamma_{th} \end{cases} \quad (1)$$

where γ is the received SNR and γ_{th} is the threshold value. The average BLER of the threshold receiver (1) in a fading channel is

$$\bar{P}_e(\bar{\gamma}) = \int_0^{\infty} P_e(\gamma) f(\gamma; \bar{\gamma}) d\gamma = F(\gamma_{th}; \bar{\gamma}) \quad (2)$$

where $\bar{\gamma}$ represents the average γ , f and F denote the probability density function (PDF) and the cumulative distribution function (CDF) of γ for a given $\bar{\gamma}$, respectively. Equation (2) implies, with powerful channel coding, the average BLER in a fading channel can be well approximated by the outage probability of the fading channel. As a result, we use CDF and BLER interchangeably in this communication.

The spatial multiplexing throughput of MIMO system with fixed modulation and coding scheme (MCS) can be simply modeled as [6]

$$T_{\text{put}}(\bar{\gamma}) = \frac{T_{\text{put,max}}}{N_t} \sum_{i=1}^{N_t} (1 - \bar{P}_e(\bar{\gamma}_i)) \quad (3)$$

where $T_{\text{put,max}}$ denotes the maximum throughput, $\bar{\gamma} = \sum_i \bar{\gamma}_i$ and N_t is the number of transmit antennas. Note that for sake of easy exhibition, we use relative throughput, defined as the throughput normalized by its maximum value, $T = T_{\text{put}}/T_{\text{put,max}}$, hereafter.

The orthogonal frequency-division multiplexing (OFDM) system effectively partitions the system bandwidth into subcarriers each experi-

ences a flat fading channel. The MIMO channel for the k th OFDM subcarrier can be modeled as

$$\mathbf{y}_k = \mathbf{H}_k \mathbf{x}_k + \mathbf{n}_k \quad (4)$$

where \mathbf{H}_k is the $N_r \times N_t$ MIMO channel, \mathbf{x}_k and \mathbf{y}_k are the $N_t \times 1$ transmit and $N_r \times 1$ receive signal vectors, respectively, and \mathbf{n} is the i.i.d. Gaussian noise vector, all at the k th subcarrier. The number of independent subcarriers can be estimated as the ratio of the system bandwidth to the coherence bandwidth; and the throughput in a selective fading channel can be obtained by coherently combining the independent subcarriers. For notational convenience, we drop the subscript k hereafter.

It has been shown that the Kronecker model [12] is as accurate as the full-correlation model [12] in an RC due to its rich scattering property [13]. Therefore, the Kronecker model is used in this work:

$$\mathbf{H} = \mathbf{R}_r^{\frac{1}{2}} \mathbf{H}_w \mathbf{R}_t^{\frac{1}{2}} \quad (5)$$

where \mathbf{H}_w denotes the spatially white $N_r \times N_t$ MIMO channel with i.i.d. complex Gaussian elements, \mathbf{R}_t and \mathbf{R}_r are $N_t \times N_t$ and $N_r \times N_r$ correlation matrices at transmit and receive sides, respectively.

In a frequency division duplex (FDD) system as in most of the current LTE systems, the transmitter uses codebook-based precoding [7], $\mathbf{x} = \mathbf{F}\mathbf{s}$, where \mathbf{s} is the transmit signal vector before precoding and \mathbf{F} is the precoding matrix. MMSE equalizers are implemented in LTE transceivers [7]. The MMSE equalizer finds a filtering matrix \mathbf{G} that minimizes $\|\mathbf{G}\mathbf{y} - \mathbf{s}\|_2^2$. \mathbf{G} can be easily derived using the orthogonality principle [12],

$$\mathbf{G} = \left(\mathbf{F}^H \mathbf{H}^H \mathbf{H} \mathbf{F} + \frac{1}{\bar{\gamma}_0} \mathbf{I} \right)^{-1} \mathbf{F}^H \mathbf{H}^H \quad (6)$$

where $\bar{\gamma}_0 = E[|x_i|^2]/E[|n_i|^2]$.

Note that the MIMO throughput modeling so far is not limited to any MIMO size. However, current OTA tests of MIMO systems are limited to 2×2 MIMO systems due to the fact that the current communication tester (i.e., the base station emulator) has only two antenna ports and that the LTE phone is equipped with two antenna ports for MIMO communications. As a result, we choose the two-antenna codebook based on 2-bit feedback [7] for modeling the closed-loop 2×2 MIMO throughput: the receiver feedbacks two bits to the transmitter; based on the two bits, the transmitter chooses a precoding matrix \mathbf{F} from the following codebook [7]:

$$\begin{bmatrix} 1 & 0 \\ 0 & 1 \end{bmatrix}, \quad \frac{1}{\sqrt{2}} \begin{bmatrix} 1 & 1 \\ 1 & -1 \end{bmatrix}, \quad \frac{1}{\sqrt{2}} \begin{bmatrix} 1 & 1 \\ j & -j \end{bmatrix}. \quad (7)$$

The selection criterion of \mathbf{F} is the trace of the weighed mean square error (MSE) matrix [9],

$$\varepsilon(\mathbf{G}, \mathbf{F}) = \text{tr} \left\{ E \left[\left\| \mathbf{W}^{\frac{1}{2}} (\mathbf{G}\mathbf{y} - \mathbf{s}) \right\|_2^2 \right] \right\} \quad (8)$$

where \mathbf{W} is the weighting matrix on the error vector $\mathbf{G}\mathbf{y} - \mathbf{s}$ and the expectation is taken over the random \mathbf{s} and \mathbf{n} . Note that \mathbf{F} is implicitly included in \mathbf{y} in (8).

For a fixed MCS and multiplexing gain, $\mathbf{W} = \mathbf{\Lambda}^{-1}$ (where $\mathbf{\Lambda}$ is a diagonal matrix consisting the eigenvalues of $\mathbf{H}^H \mathbf{H}$) should be used to ensure equal BLERs among all the streams [9]. Intuitively, the weighting matrix $\mathbf{\Lambda}^{-1}$ puts more weight on the larger error and less weight on the smaller one in selecting \mathbf{F} to ensure equal errors among the streams. Substituting (6) and $\mathbf{W} = \mathbf{\Lambda}^{-1}$ into (8), one obtains

$$\varepsilon(\mathbf{F}) = \text{tr} \left[\mathbf{\Lambda}^{-1} (\mathbf{I} + \bar{\gamma}_0 \mathbf{F}^H \mathbf{H}^H \mathbf{H} \mathbf{F})^{-1} \right] \quad (9)$$

the derivation of which is shown in the Appendix.

Note that the well-known (unweighted) MSE $\mathbf{W} = \mathbf{I}$ minimizes the sum of the BLERs of all the streams, yet it does not guarantee the BLER of each individual stream; the weight $\mathbf{W} = \mathbf{\Lambda}$ is optimal for the mutual information in a MIMO system that support arbitrary bit loading among the spatial streams [9]. In LTE spatial multiplexing systems, however, the bits are equally loaded in all streams. Thus, $\mathbf{W} = \mathbf{\Lambda}$ is not a good criterion for the precoding in LTE systems. The performances of different MSE criteria are compared in Section III.

Left multiplying \mathbf{G} (6) to both sides of (4), the MMSE SNR can be readily derived as

$$\gamma_i = \frac{1}{[(\bar{\gamma}_0 \mathbf{F}^H \mathbf{H}^H \mathbf{H} \mathbf{F} + \mathbf{I})^{-1}]_{i,i}} - 1. \quad (10)$$

Note that in this communication we do not distinguish the SNR and the signal to interference and noise ratio (SINR) in that the inter-stream interference is considered as noise.

In an open-loop MIMO system, the throughput model is the same by choosing $\mathbf{F} = \mathbf{I}$. In Section IV, we compare the measured open- and closed-loop MIMO throughputs of the same LTE mobile phone.

III. SIMULATIONS

In order to test the mobile phone alone in the downlink mode, most OTA tests are conducted in the receive semi-correlation setup, i.e., the mobile phone under test (with correlated antennas) are measured as the receiver; the antennas at the base station (transmitter) are uncorrelated. However, as shown in the sequel of this communication, correlations at the transmit side has a great impact on the throughput performance of the LTE phone, especially for the closed-loop MIMO system.

For simplicity, we assume flat fading channel in this section. We first generate 10 000 channel snapshots. Based on the channel snapshots, instantaneous SNR samples are gathered in open- and closed-loop configurations, respectively; and the corresponding empirical CDF is obtained using the 10 000 SNR samples. Once the average BLER is obtained, the MIMO throughput can be calculated easily using (3).

We consider a 2×2 MIMO system in both open- and closed-loop configurations. Fig. 1 shows the throughputs of the open- and closed-loop MIMO systems for both receive and transmit semi-correlation case. In addition to the weighted MSE criterion (9) with the weighting matrix $\mathbf{W} = \mathbf{\Lambda}^{-1}$, the other two MSE criteria with weighting matrices $\mathbf{W} = \mathbf{I}$ and $\mathbf{W} = \mathbf{\Lambda}$ (cf. Section II) are also applied in the simulations. As expected, since the unweighted MSE criterion ($\mathbf{W} = \mathbf{I}$) tends to select a precoding matrix \mathbf{F} that minimizes the sum of the BLERs of two streams, the BLER of the worst stream is not guaranteed; since the other weighted MSE criterion ($\mathbf{W} = \mathbf{\Lambda}$) tends to select a precoding matrix \mathbf{F} that minimizes the BLER of best stream, the resulting throughput performance is limited by the worst stream, making it inferior to the other two criterion. As can be seen, when the correlation exists only at the transmit side (Tx), precoding with the weighted MSE criterion (11) improves the throughput at low SNR. At high SNR with large correlation (e.g., 0.9) at the transmit side, precoding (closed-loop) based on the 2-bit feedback even yields slightly worse throughput performance than the open-loop case. This seemingly surprising observation makes sense because, unlike the low SNR case, at high SNR the channel estimation error from the 2-bit feedback starts to affect the throughput performance adversely and the number of feedback bits should be proportional to the SNR for the precoding to be useful [10]. When the correlation exists only at the receive side (Rx), precoding has little effect on the throughput. For the general case where correlations exist at both MIMO ends, the precoding is effective as long as the correlation at the transmit side is significant (cf. Section IV).

IV. MEASUREMENTS

To validate the throughput model, the throughputs of an LTE mobile phone in both open- and closed configurations are measured in an

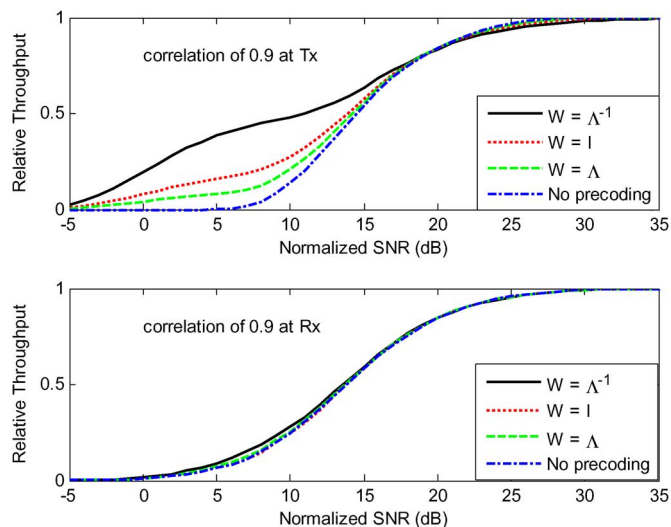


Fig. 1. Relative throughputs of 2×2 open- and closed-loop LTE MIMO systems. The upper graphs correspond to the transmit semi-correlation case; the lower graphs correspond to the receive semi-correlation case. The normalized SNR is defined $\bar{\gamma}/(\gamma_{th} \bar{\gamma}_0)$ [6].

RC. A commercial communication tester is used as the LTE base station. The commercial LTE mobile phone with external antenna ports for OTA tests is measured as the receiver. In order to study the antenna impairment on the throughput, the LTE phone was connected to the good CTIA reference antenna and the base station was connected to the bad CTIA reference antenna. The characteristics of the CTIA reference antennas can be readily determined from passive measurements in the RC: the magnitudes of the complex antenna correlations of the good, nominal, and bad CTIA reference antennas are about 0.13, 0.57, and 0.90, respectively; the antenna efficiencies of the good, nominal, and bad CTIA reference antennas are about -1.4 , -3.1 , and -4.0 dB, respectively. Measurements of the LTE phone were performed on the LTE band 13, i.e., 751 MHz, with 10 MHz system bandwidth in closed-loop configuration. The fixed MCS index 20 and a resource block (RB) of 50 were chosen in the communication tester.

During the measurement, the RC was loaded to achieve a RMS delay spread of 90 ns (corresponding to 3 MHz coherence bandwidth). The OFDM effectively partition the wideband channel into subcarrier channels each experience a Rayleigh-flat fading in the RC. Intuitively the number of independent subcarrier channels can be approximated by dividing the system bandwidth (10 MHz) by the coherence bandwidth (3 MHz), resulting a 3-order frequency diversity.

Note that only absolute power values are available from the OTA testing instruments. Thus, the measured throughputs are shown as a function of average received power \bar{P} . In simulations, the relative throughput is presented as a function of normalized SNR. To compare the modeled relative throughput with the measured one, we need to correct the x-axis of the simulated curve with the absolute threshold value P_{th} , $P_{th} \bar{\gamma}_0 / \bar{\gamma}$. The threshold value P_{th} was obtained from the conductive measurement (i.e., the transmitter and receiver are connected via RF cables) with the same system settings. The threshold value is read out from the half of the conductive throughput. For the sake of conciseness, the conductive measurement results are not shown in this communication.

Fig. 2 shows the measured and modeled relative throughputs for the 2×2 open- and closed-loop MIMO systems. Good agreements between the measure and modeled throughputs are observed. Note that, due to the high correlation (e.g., 0.9) at the transmit side, the throughput of the closed-loop MIMO system is much larger than that of the open-loop MIMO system in the lower SNR (power) regime and lower than

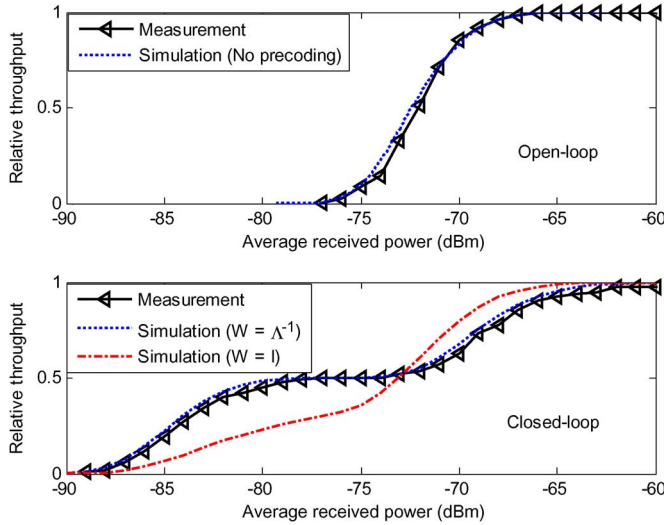


Fig. 2. Measured and modeled throughputs for the 2×2 open- and closed-loop MIMO systems.

that of the open-loop MIMO system in the higher SNR regime. These observations are intuitive: at low SNR, the throughput (or BLER) performance is limited by the worst stream, thus the weighted precoding ($\mathbf{W} = \mathbf{\Lambda}^{-1}$) improves the MIMO throughput by putting more effort in improving the worst stream; at high SNR, the BLERs of both streams are good enough, precoding can only be helpful with more accurate estimation of the channel (i.e., more feedback bits than the 2-bit feedback are required) [10].

V. CONCLUSION

In this communication, we present the throughput model for the closed-loop 2×2 MIMO system with 2-bit feedback. The weighted MSE selection criterion for precoding is derived. There are good agreements between the modeled and measured throughputs. Simulation and measurement results indicate that the codebook-based precoding based on the 2-bit feedback in LTE systems is useful at low and medium SNRs with high correlations at the transmit side. Remarkably, it is shown that the precoding based on the 2-bit feedback (closed-loop) yields worse throughput performance than the open-loop case at high SNR with high correlations at the transmit side.

APPENDIX DERIVATION OF (9)

Let $\mathbf{e} = \mathbf{G}\mathbf{y} - \mathbf{s}$ and $\mathbf{W} = \mathbf{\Lambda}^{-1}$ (a real-valued diagonal matrix), (8) can be rewritten as

$$\begin{aligned}
 \varepsilon(\mathbf{G}, \mathbf{F}) &= \text{tr} \left\{ E[\mathbf{\Lambda}^{-1/2} \mathbf{e} \mathbf{e}^H \mathbf{\Lambda}^{-1/2}] \right\} \\
 &= \text{tr} \left\{ E[\mathbf{\Lambda}^{-1} \mathbf{e} \mathbf{e}^H] \right\} \\
 &= \text{tr} \left\{ E \left[\mathbf{\Lambda}^{-1} \mathbf{e} (\mathbf{G}\mathbf{y} - \mathbf{s})^H \right] \right\} \\
 &= \text{tr} \left\{ E \left[\mathbf{\Lambda}^{-1} (\mathbf{G}\mathbf{y} - \mathbf{s}) \mathbf{s}^H \right] \right\} \\
 &= \text{tr} \left\{ \mathbf{\Lambda}^{-1} \left(\mathbf{G} E \left[(\mathbf{H}\mathbf{F}\mathbf{s} + \mathbf{n}) \mathbf{s}^H \right] - E[\mathbf{s}\mathbf{s}^H] \right) \right\} \\
 &= \text{tr} \left[\mathbf{\Lambda}^{-1} (\mathbf{G}\mathbf{H}\mathbf{F} - \bar{\gamma}_0 \mathbf{I}) \right] \\
 &= \text{tr} \left\{ \mathbf{\Lambda}^{-1} \left[\left(\mathbf{F}^H \mathbf{H}^H \mathbf{H}\mathbf{F} + \frac{1}{\bar{\gamma}_0} \mathbf{I} \right)^{-1} \mathbf{F}^H \mathbf{H}^H \mathbf{H}\mathbf{F} - \bar{\gamma}_0 \mathbf{I} \right] \right\} \\
 &= \text{tr} \left[\mathbf{\Lambda}^{-1} (\mathbf{I} + \bar{\gamma}_0 \mathbf{F}^H \mathbf{H}^H \mathbf{H}\mathbf{F})^{-1} \right].
 \end{aligned}$$

The second equality is due to the property of the trace operator that $\text{tr}[\mathbf{A}\mathbf{B}] = \text{tr}[\mathbf{B}\mathbf{A}]$ for an $m \times n$ matrix \mathbf{A} and an $n \times m$ matrix \mathbf{B} . The fourth equality follows the orthogonality principle of the MMSE that $E[\mathbf{e}\mathbf{y}^H] = \mathbf{0}$ (e.g. [12]). The derivation is also based on the assumption that the transmit signals (before precoding) are uncorrelated and there is no correlation between the transmitted signal and the white Gaussian noise with unity variance: $E[\mathbf{s}\mathbf{s}^H] = \bar{\gamma}_0 \mathbf{I}$ and $E[\mathbf{n}\mathbf{s}^H] = \mathbf{0}$. The last equality follows the Sherman-Morrison-Woodbury formula [14]: $(\mathbf{A} + \mathbf{B}\mathbf{D}\mathbf{C})^{-1} = \mathbf{A}^{-1} - \mathbf{A}^{-1}\mathbf{B}(\mathbf{D}^{-1} + \mathbf{C}\mathbf{A}^{-1}\mathbf{B})\mathbf{C}\mathbf{A}^{-1}$.

REFERENCES

- [1] E. Genender, C. L. Holloway, and K. A. Remley *et al.*, "Simulating the multipath channel with a reverberation chamber: Application to bit error rate measurements," *IEEE Trans. Electromagn. Compat.*, vol. 52, pp. 766–777, 2010.
- [2] G. Ferrara, M. Migliaccio, and A. Sorrentino, "Characterization of GSM non-line-of-sight propagation channels generated in a reverberating chamber by using bit error rates," *IEEE Trans. Electromagn. Compat.*, vol. 49, no. 3, pp. 467–473, Aug. 2007.
- [3] M. A. García-Fernández, J. D. Sánchez-Heredia, and A. M. Martínez-González *et al.*, "Advances in mode-stirred reverberation chambers for wireless communication performance evaluation," *IEEE Commun. Mag.*, vol. 49, no. 7, pp. 140–147, Jul. 2011.
- [4] R. Recanatini, F. Moglie, and V. Mariani Primiani, "Performance and immunity evaluation of complete WLAN systems in a large reverberation chamber," *IEEE Trans. Electromagn. Compat.*, vol. 55, no. 5, pp. 806–815, Oct. 2013.
- [5] N. Arsalane, M. Mouhamadou, and C. Decroze *et al.*, "3GPP channel model emulation with analysis of MIMO-LTE performances in reverberation chamber," *Int. J. Antennas Propag.*, 2012 [Online]. Available: <http://dx.doi.org/10.1155/2012/239420>, Article ID 239420, 8 pages
- [6] X. Chen, "Throughput modeling and measurement in an isotropic-scattering reverberation chamber," *IEEE Trans. Antennas Propag.*, vol. 62, no. 4, pp. 2130–2139, April 2014.
- [7] LTE Physical Layer—General Description 3rd Generation Partnership Project, Tech. Rep. TS 36201, Nov. 2007, V8.1.0.
- [8] I. Szini, Reference antenna proposal for MIMO OTA, CTIA Contribution MOSG110504R1., May 2011.
- [9] H. Sampath, P. Stoica, and A. Paulraj, "Generalized linear precoder and decoder design for MIMO channels using the weighted MMSE criterion," *IEEE Trans. Commun.*, vol. 49, no. 12, pp. 2198–2206, Dec. 2001.
- [10] D. J. Love and R. W. Heath, "Limited feedback unitary precoding for spatial multiplexing system," *IEEE Trans. Inf. Theory*, vol. 51, no. 8, pp. 2967–2976, Aug. 2005.
- [11] M. R. D. Rodrigues, I. Chatzigeorgiou, I. J. Wassell, and R. Carrasco, "Performance analysis of turbo codes in quasi-static fading channels," *IET Commun.*, vol. 2, no. 3, pp. 449–461, 2008.
- [12] A. Paulraj, R. Nabar, and D. Gore, *Introduction to Space-Time Wireless Communication*. Cambridge, U.K.: Cambridge Univ. Press, 2003.
- [13] X. Chen, "Spatial correlation and ergodic capacity of MIMO channel in reverberation chamber," *Int. J. Antennas Propag.*, 2012, Article ID 939104, 7 pages.
- [14] A. J. Laub, *Matrix Analysis for Scientists and Engineers*. Philadelphia, PA, USA: SIAM, 2005.